



**4th International Conference on
Numerical and Symbolic Computation
Developments and Applications**

PROCEEDINGS

April, 11 - 12,

ISEP – Instituto Superior de Engenharia do Porto

PORTO, Portugal





4th International Conference on Numerical and Symbolic Computation: Developments and Applications.

April, 11- 12, 2019, ISEP, Porto, Portugal, ©ECCOMAS.

ISBN: : 978-989-99410-5-2;

SYMCOMP 2019 – 4th International Conference on Numerical and Symbolic Computation:
Developments and Applications

Edited by APMTAC – Associação Portuguesa de Mecânica Teórica, Aplicada e Computacional

Editors: Maria Amélia Loja (IDMEC, ISEL/CIMOSM), Joaquim Infante Barbosa (IDMEC, ISEL/CIMOSM),
José Alberto Rodrigues (ISEL/CIMOSM) e Paulo B. Vasconcelos (CMUP/FEP-UP)

April, 2019





1 – Introduction

The Organizing Committee of SYMCOMP2019 – 4th International Conference on Numerical and Symbolic Computation: Developments and Applications, welcomes all the participants and acknowledge the contribution of the authors to the success of this event.

This fourth International Conference on Numerical and Symbolic Computation, is promoted by APMTAC - Associação Portuguesa de Mecânica Teórica, Aplicada e Computacional and it was organized in the context of IDMEC - Instituto de Engenharia Mecânica, Instituto Superior Técnico, Universidade de Lisboa. With this ECCOMAS Thematic Conference it is intended to bring together academic and scientific communities that are involved with Numerical and Symbolic Computation in the most various scientific areas

SYMCOMP 2019 elects as main goals:

To establish the state of the art and point out innovative applications and guidelines on the use of Numerical and Symbolic Computation in the numerous fields of Knowledge, such as Engineering, Physics, Mathematics, Economy and Management, Architecture, ...

To promote the exchange of experiences and ideas and the dissemination of works developed within the wide scope of Numerical and Symbolic Computation.

To encourage the participation of young researchers in scientific conferences.

To facilitate the meeting of APMTAC members (Portuguese Society for Theoretical, Applied and Computational Mechanics) and other scientific organizations members dedicated to computation, and to encourage new memberships.

We invite all participants to keep a proactive attitude and dialoguing, exchanging and promoting ideas, discussing research topics presented and looking for new ways and possible partnerships to work to develop in the future.

The Executive Committee of SYMCOMP2019 wishes to express his gratitude for the cooperation of all colleagues involved in various committees, the Scientific Committee, the Programm Committee, Organizing Committee and the Secretariat. We hope everyone has enjoyed helping to consolidate this project, which we are sure will continue in the future. Our thanks to you all.

- Amélia Loja, Chairperson (IDMEC/LAETA, CIMOSM/ISEL)
- Paulo B. Vasconcelos, Chairperson (CMUP/FEP-UP)
- António J. M. Ferreira (FEUP/INEGI)
- Joaquim Infante Barbosa (IDMEC/LAETA, CIMOSM/ISEL)
- José Alberto Rodrigues (CIMOSM, ADM/ISEL)



2 – CONFERENCE BOARD

Chairperson

Maria Amélia Ramos Loja, ISEL/CIMOSM ; IDMEC/LAETA

Instituto Superior de Engenharia de Lisboa

Rua Conselheiro Emídio Navarro, 1, 1959-007 Lisboa

Email : amelialoja@dem.isel.ipl.pt, amelialoja@tecnico.ulisboa.pt

Chairperson

Paulo José Abreu Beleza de Vasconcelos, (CMUP/FEP-UP)

Centro de Matemática da Universidade do Porto (CMUP)

Rua do Campo Alegre, 687, 4169-007 Porto, Portugal

Email : pjv@fep.up.pt

EXECUTIVE COMMITTEE

- Amélia Loja (IDMEC/LAETA, ISEL/CIMOSM)
- Joaquim Infante Barbosa (IDMEC/LAETA, ISEL/CIMOSM)
- José Alberto Rodrigues (ISEL/CIMOSM)
- Inês Carvalho Jerónimo Barbosa (ISEL/CIMOSM)

ORGANIZING COMMITTEE

Amélia Loja, Chairperson (IDMEC, CIMOSM)

Paulo B. Vasconcelos, Chairperson (CMUP/FEP-UP)

António J. M. Ferreira (FEUP/INEGI)

Joaquim Infante Barbosa (IDMEC, CIMOSM)

José Alberto Rodrigues (CIMOSM, ADM/ISEL)

LOCAL ORGANIZING COMMITTEE

Amélia Caldeira (SYSTEC/ISR, LEMA/ISEP-IPP)

José Estrela da Silva (ISEP/IPP)

Manuel Cruz (LEMA/ISEP-IPP)

Paulo B. Vasconcelos (CMUP/FEP-UP)



SCIENTIFIC COMMITTEE

Alexandre Francisco (IST, INESC-IDC, Lisboa, Portugal)	José Luis López-Bonilla (SSMEE, National Polytechnic Institute, Mexico)
Amélia Loja (IDMEC/IST, CIMOSM/ISEL, Lisboa, Portugal)	José Miranda Guedes (IDMEC/IST, Lisboa, Portugal)
Ana Conceição (Universidade do Algarve, Faro, Portugal)	José Eugénio S Garção (Universidade de Évora, Portugal)
Ana Neves (FEUP, Porto, Portugal)	Juan Nuñez (University of Sevilla, Spain)
António J M Ferreira (FEUP, Porto, Portugal)	Krassimir Atanassov (Institute of Biophysics and Biomedical Engineering, Bulgarian Academy of Sciences, Sofia, Bulgaria)
Antonio Tornambe (Universita di Roma Tor Vergata, Italy)	Lina Vieira (ESTeSL/IPL, Lisboa, Portugal)
Aurélio Araújo (IDMEC/IST, Lisboa, Portugal)	Lorenzo Dozio (Politecnico di Milano, Italy)
Bican Xia (LMAM & School of Mathematical Sciences, Peking University, China)	Luís Durão (CIDEM/ISEP-IPP, Porto, Portugal)
Carlos A. Mota Soares (IDMEC/IST, Lisboa, Portugal)	María Barbero Liñán (Universidad Politécnica de Madrid / ICMAT (CSIC-UAM-UC3M), Spain)
Christopher Peterson (Colorado State University, USA)	Miguel Matos Neves (IDMEC/IST, Lisboa, Portugal)
Cristóvão M Mota Soares (IDMEC/IST, Lisboa, Portugal)	Nicholas Fantuzzi (Bologna University, Italy)
Dongming Wang (Beihang University, Beijing, China and CNRS, Paris, France)	Oliver Schuetze (CINVESTAV-IPN, Mexico)
Eduardo Ortiz (Imperial College, London, UK)	Osni Marques (Lawrence Berkeley National Laboratory, USA)
Francesco Tornabene (Alma Mater Studiorum, University of Bologna, Italy)	Paulo B. Vasconcelos (CMUP/FEP - Porto, Portugal)
Francisco Marcellán Español (Universidad Carlos III de Madrid, Spain)	Paulo Rebelo (UBI - Universidade da Beira Interior, Covilhã, Portugal)
Gianluigi Rozza (SISSA, Mathematics Area, International School for Advanced Studies, Italy)	Pedro Areias (Universidade de Évora, Portugal)
Hélder Carriço Rodrigues (IDMEC/IST, Lisboa, Portugal)	Piotr Luszek (University of Tennessee, Knoxville, USA)
Ilias Kotsireas (Wilfrid Laurier University, Toronto, Canada)	Silvério Rosa (UBI - Universidade da Beira Interior, Covilhã, Portugal)
J.N. Reddy (Texas A&M University, USA)	Stéphane Louis Clain (CMAT – Universidade do Minho, Portugal)
Joaquim Infante Barbosa (IDMEC/IST, CIMOSM/ISEL, Lisboa, Portugal)	Subhas Chandra Kattimani (National Institute of Technology Karnataka, Surathkal, India)
José Alberto Rodrigues (CIMOSM/ISEL, Lisboa, Portugal)	Rachid Touzani (Laboratoire de Mathématiques Blaise Pascal, Polytech Clermont-Ferrand, France)
José Andrade Matos (CMUP/ISEP-IPP, Porto, Portugal)	Vinyas Mahesh (Nitte Meenakshi Institute of Technology, Bangalore, India)
José Carlos Santos (FCUP, Porto, Portugal)	Xesús Nogueira (Civil Engineering School, Universidad da Coruna, Spain)



Programme Committee

Alda Carvalho (CIMOSM-ISEL, CEMAPRE)	Luís Durão (CIDEM/ISEP-IPP)
Amélia Caldeira (SYSTEC/ISR, LEMA/ISEP-IPP)	Olympia Roeva (Institute of Biophysics and Biomedical Engineering, Bulgarian Academy of Sciences)
Ana Conceição (Universidade do Algarve)	Paula V. Martins (FCT-UALG, CIEO)
Ângela Macedo (CMUP, UTAD)	Paulo A. G. Piloto (INEGI, IPB)
Eliana Oliveira da Costa e Silva (ESTG-IPP, CIICESI)	Paulo B. Vasconcelos (CMUP/FEP-UP)
Elza M. M. Fonseca (INEGI, ISEP/IPP)	Renato M. Natal Jorge (INEGI, FEUP)
Evdokia Sotirova (Intelligent Systems Laboratory, University “Prof. Dr. Asen Zlatarov”)	Rui Borges Lopes (DEGEIT-UA, CIDMA)
Fernando Fontes (SYSTEC ISR, FEUP UP)	Sílvia Barbeiro (CMUC/FCTUC-UC)
Jorge Belinha (INEGI, ISEP-IPP)	Sofia Lopes (SYSTEC ISR, CFIS UMINHO)
Jorge Andraz (FE-UALG, CEFAGE)	Tiago Silva (UNIDEMI, FCT/UNL, CIMOSM/ISEL)
José Matos (CMUP – ISEP)	Zélia Rocha (CMUP, FCUP)

SPONSORS

ECCOMAS – European Community on Computational Methods in Applied Sciences

APMTAC – Associação Portuguesa de Mecânica Teórica, Aplicada e Computacional, (Portuguese Society for Theoretical, Applied and Computational Mechanics), ECCOMAS Member Association;

IDMEC/LAETA – Instituto de Engenharia Mecânica/Laboratório Associado de Energia, Transportes e Aeronáutica (Mechanical Engineering Institute/Associated Laboratory for Energy, Transportes and Aeronautics);

ISEL/IPL – Instituto Superior de Engenharia de Lisboa, Instituto Politécnico de Lisboa

CMUP—Centro de Matemática da Universidade do Porto

LEMA, ISEP– Laboratório de Engenharia Matemática, Instituto Superior de Engenharia do Porto

WOLFRAM RESEARCH



4th International Conference on Numerical and Symbolic Computation: Developments and Applications.

April, 11- 12, 2019, ISEP, Porto, Portugal, ©ECCOMAS.

ORGANIZING INSTITUTION

IDMEC/LAETA – Instituto de Engenharia Mecânica/Laboratório Associado de Energia, Transportes e Aeronáutica.

PLACE OF THE EVENT

ISEP – Instituto Superior de Engenharia do Porto

Rua Dr. António Bernardino de Almeida, 431, Porto

(**Building E**)

Contents

INTRODUCTION	i
CONTENTS	vii
ADVANCES IN GEOMETRY INDEPENDENT APPROXIMATIONS	1
PARALLEL SOLUTION OF LARGE-SCALE LINEAR AND NON-LINEAR EIGENVALUE PROBLEMS WITH SLEPc	5
KINEMATICS OF A CLASSICAL BALLET BASE MOVEMENT USING A KINETIC SENSOR	7
FIRE PERFORMANCE OF PARTIALLY ENCASED COLUMN SUBJECTED TO ECCENTRIC LOADING	17
NUMERICAL SIMULATIONS OF INDUSTRIAL SEEL PORTAL FRAMES UNDER FIRE CONDITIONS	27
AEROELASTIC WING ANALYSIS AND DESIGN	41
DESIGN FOR CRASHWORTHINESS OF AN ELECTRIC VEHICLE	61
ORTHOGONAL POLYNOMIALS WITH ULTRA-EXPONENTIAL WEIGHT FUNCTIONS: AN EXPLICIT SOLUTION TO THE DITKIN-PRUDNIKOV PROBLEM	81
HADAMARD-GERSHGORIN LOCATION OF ZEROS, LOCATION OF EXTREMAL ZEROS AND SOME RESULTS ON FIXED POINTS OF PERTURBED CHEBYSHEV POLYNOMIALS OF SECOND KIND	83
STABLE EVALUATION OF GAUSSIAN KERNEL APPLIED TO INTERFACE PROBLEMS	85

ON SOME RBF COLLOCATION METHODS IN THE APPLI- CATION TO PROBLEMS WITH DISCONTINUITY	97
FIRE SAFETY OF WOOD-STEEL CONNECTIONS	109
CRITICAL TEMPERATURE FOR THE COMPONENTS OF COM- POSITE SLABS WITH STEEL DECK UNDER FIRE FOR LOAD-BEARING RATING	119
THE CONTINUOUS WAVELET TRANSFORM IN ECONOMICS AND THE ASTOOLBOX	137
EVALUATING AND FACTORING QUATERNIONIC POLYNO- MIALS	139
SYMBOLIC COMPUTATIONS OVER THE ALGEBRA OF CO- QUATERNIONS	141
ON A 2-ORTHOGONAL POLYNOMIAL SEQUENCE VIA QUADRATIC DECOMPOSITION	157
ESTIMATING THE ‘EMPLOYMENT BAND OF INACTION’ WITH MULTIPLE BREAKS DUE TO LABOUR MARKET REFORMS	159
VARIABLE PRECISION TO ENSURE HIGH ACCURACY IN SPECTRAL METHODS	173
ROBUSTNESS OF A NEURO-GENETIC PID CONTROLLERS AUTO-TUNING	181
A DEEPER LOOK IN THE INTERCRITERIA POSITIVE CON- SONANCE BETWEEN THE BUSINESS SOPHISTICATION AND INNOVATION PILLARS OF COMPETITIVENESS IN THE EUROPEAN UNION IN 2015-2018	199
INTERCRITERIA ANALYSIS OF FOREST FIRE RISK	215
EXPLICIT FORMULAE FOR DERIVATIVES AND PRIMITIVES OF ORTHOGONAL POLYNOMIALS	231
EUROPEAN UNION MEMBER STATES’ PERFORMANCE IN THE 2018 GLOBAL COMPETITIVENESS INDEX 4.0 THROUGH THE PRISM OF INTERCRITERIA ANALYSIS	251
(ALMOST) EXACT COMPUTATION OF DIFFERENTIAL EIGEN- VALUES IN APPROXIMATE PROBLEMS	263

DYNAMIC EFFECTS OF INTERNATIONAL TRADE UNDER IMPERFECT COMPETITION AND ECONOMIES OF SCALE	273
ROBUST ORTHOGONAL PADE APPROXIMATION	293
COMPUTING THE KERNEL OF SPECIAL CLASSES OF PAIRED SINGULAR INTEGRAL OPERATORS WITH MATHEMAT- ICA SOFTWARE	301
DYNAMIC AND INTERACTIVE MATHEMATICAL TOOLS IN SOCIO-ECONOMIC SCIENCES CLASSROOMS	321
APPLICATION OF MULTIDIMENSIONAL HERMITE POLY- NOMIALS TO FLUID MECHANICS	337
AN INTERACTIVE WAY OF ANALYZING ECONOMIC CON- CEPTS USING SYMBOLIC COMPUTATION	343
COOPERATION BETWEEN FEATURE SELECTION METH- ODS IN THE CONTEXT OF A SUPERVISED MACHINE LEARNING TASK	357
SYMBOLIC AND NUMERICAL TECHNIQUES FOR DETER- MINING CUBATURE RULES ON THE TRIANGLE	359
FACTOR DISTRIBUTION MEETS INDUSTRIAL ORGANIZA- TION: THE LABOR SHARE'S BEHAVIOR UNDER A NEO- SCHUMPETERIAN ENVIRONMENT	361
AN IMPROVED INTUITIONISTIC FUZZY ESTIMATION OF THE AREA OF 2D-FIGURES BASED ON THE PICK'S FOR- MULA	363
SLIP FLOWS OF GENERALISED PHAN-THIEN-TANNER FLU- IDS: ANALYTICAL AND NUMERICAL STUDIES	375
A VISUAL EXPLORATION TOOL FOR MULTI-OBJECTIVE MIXED INTEGER OPTIMIZATION	377
APPLICATION OF THE GAME METHOD FOR MODELLING FOR LOCATING THE WILDFIRE IGNITION POINT	397
THE RPIM FOR THE ELASTO-PLASTIC ANALYSIS OF MA- TERIALS USING A MODIFIED HILL YIELD CRITERION	415
MODELS AND NUMERICAL METHODS FOR MARINE VE- HICLES TRAJECTORY OPTIMIZATION	417

NUMERICAL METHODS FOR DELAYED OPTIMAL CONTROL PROBLEMS	435
COMPUTATIONAL MODEL OF BONE'S ADAPTATION TO A MECHANICAL STIMULUS CONSIDERING CELLULAR DYNAMICS	437
SCHUR AND CHEBYSHEV EXPANSIONS OF REPRODUCING KERNELS	439
A FABRIC TENSOR BASED 3D HOMOGENIZATION TECHNIQUE FOR THE MECHANICAL CHARACTERIZATION OF TRABECULAR BONE TISSUE	441
MULTI-OBJECTIVE FEATURE SELECTION BASED ON GENETIC ALGORITHMS FOR CLASSIFICATION PROBLEMS	443
NEURAL NETWORK CLASSIFIERS FOR PULSE SHAPE ANALYSIS	445
HIGH PERFORMANCE COMPUTATION WITH ADI ON CARTESIAN GRID TO SOLVE THE STEADY STATE 2D CONVECTION DIFFUSION EQUATION	447
ADVANCED DISCRETIZATION TECHNIQUES IN COMPUTATIONAL MECHANICS AND BIOMECHANICS	457
A DECISION MODEL FOR THE LOCATION OF SOLID URBAN WASTE TRANSFER STATIONS IN THE COUNTY OF FELGUEIRAS	477
SOLUTION OF CONTROL NONHOLONOMIC SYSTEMS USING SPECTRAL METHODS	479
MOVING AVERAGES AS RANDOM FOREST FEATURES TO IMPROVE SHORT-TERM WIND TURBINE POWER FORECAST	487
STUDDING ENDOTHELIAL CELL MIGRATION DUE TO CHEMOTAXIS: A NUMERICAL APPROACH	499
IMAGE RESTORATION MODELS THROUGH BACKPROPAGATION ON MEDICAL IMAGING	501
OUTSOURCING OPTIMIZATION IN SHOE INDUSTRY	503
NUMERICAL SIMULATION OF A POLYMERIC NERVE GUIDANCE CHANNEL WITH DIFFERENT GEOMETRIES	505

FACTORS FOR MARKETING INNOVATION IN PORTUGUESE FIRMS	507
INNOVATION OF GOODS AND SERVICES AND THE INFLUENCE OF ENVIRONMENTAL FACTORS	509
OPTIMAL DISTRIBUTION OF INCOME FOUND BY EVOLUTIONARY COMPUTATION	511
INTRODUCING A NEW TWO-PARAMETER INVARIANT FUNCTION FOR ALGEBRAS	517
REPLANNING THE IRRIGATION SYSTEMS	533
A NEW HP-H ADAPTIVE MESH REFINEMENT ALGORITHM FOR SOLVING OPTIMAL CONTROL PROBLEMS	541
MAGNETIC EDDY DIFFUSIVITY BY PADÉ APPROXIMATION EMPLOYING MATHEMATICA SYMBOLIC COMPUTING	543
COMPUTATIONAL SIMULATION OF BLOOD FLOW WITH CLOTS USING ADVANCED DISCRETIZATION MESHLESS METHODS	545
AN ANALYSIS OF WIND FARM DATA TO EVIDENCE LOCAL WIND PATTERN SWITCHES	547
A NUMERICAL TECHNIQUE TO SOLVE DELAYED-ADVANCED DIFFERENTIAL EQUATIONS	561
HIGH-ORDER METHODS FOR SYSTEMS OF FRACTIONAL ORDINARY DIFFERENTIAL EQUATIONS	565
DISTRIBUTED ORDER TIME-FRACTIONAL DIFFUSION: A NUMERICAL METHOD	567
USING SYMBOLIC COMPUTATION FOR FREE VIBRATION ANALYSIS OF FRAMES WITH DIFFERENT CROSS-SECTION MEMBERS	569
SPEEDING UP THE EVOLUTIONARY DATA SELECTION	571
INTERACTIONS IN A WIND FARM: A SPECTRAL ANALYSIS APPROACH	573
ISOGEOMETRIC ANALYSIS OF MECHANICAL DEFORMATION	587



S10 – CRITICAL TEMPERATURE FOR THE COMPONENTS OF COMPOSITE SLABS WITH STEEL DECK UNDER FIRE FOR LOAD-BEARING RATING

Paulo A. G. Piloto^{1*}, Carlos Balsa¹, Fernando Ribeiro², Lucas Santos³, Ronaldo Rigobello² and Érica Kimura³

1: Instituto Politécnico de Bragança
Campus Santa Apolónia, 5300-253 Bragança, Portugal
e-mail: ppiloto@ipb.pt, web: <http://www.ipb.pt>

2: Universidade Tecnológica Federal do Paraná
Campus Campo Mourão, Rod. BR 369, CEP: 87301-006, Brasil
e-mail: rigobello@utfpr.edu.br, f.freire12@gmail.com, web: <http://portal.utfpr.edu.br/>

3: Universidade Tecnológica Federal do Paraná
Campus Curitiba Ecoville, R. Deputado Heitor, Alencar Furtado, 5000 - CEP 81280-340, Brasil
e-mail: ekimura@utfpr.edu.br, lucasobmep@outlook.com, web: <http://portal.utfpr.edu.br/>

Keywords: Composite slabs with profiled steel deck, Fire, Critical temperature, Numerical validation

Abstract *Composite slabs made with concrete and steel deck are widely used in building structures. They also include other components, such as steel rebars for positive bending and a steel mesh for negative bending, preventing cracks in concrete. The fire rating of this type of elements can be determined by standard fire tests, accounting for load (R), Integrity (E) and Insulation (I). This investigation deals with the fire resistance for load (R) and insulation (I), using a numerical model validated with experimental tests. This model considers material and geometric non-linear behaviour, using perfect contact between materials. The 3D finite element mesh uses solids, shells and bars, to model a simply supported composite slab with 3.2m long, 0.65 m wide and total height of 143mm, using a trapezoidal steel deck PRINS PSV73. Different load levels are simulated (live load ranging from 1.0 kN/m² to 21 kN/m²) in addition to the dead load (2.8 kN/m²). The fire resistance (R) is determined according to standards, looking for the maximum displacement or the rate of displacement, while the fire resistance (I) looks for the average or for the maximum temperature increase at the unexposed side. The critical temperature of each steel component decreases with the load level. A new proposal is presented for the fire resistance depending on the load level.*

1. INTRODUCTION

A composite slab consists of cold-formed profiled steel deck which acts as a permanent formwork to the concrete topping. Normally, this composite solution requires the addition of other components such as steel rebars (placed within the ribs) for positive bending and steel mesh for negative bending, preventing cracks in concrete, see figure 1. Due to the external reinforcement provided by the steel deck, composite slabs generally require less additional reinforcement and less concrete as well, resulting in slender slabs. In addition, the reduction of the construction time, elimination/reduction of struts and the simplicity of installation are other advantages of composite slabs in comparison to conventional flat concrete slabs. The composite action between the concrete and the steel deck is generally achieved by indentations or embossments in the steel deck.

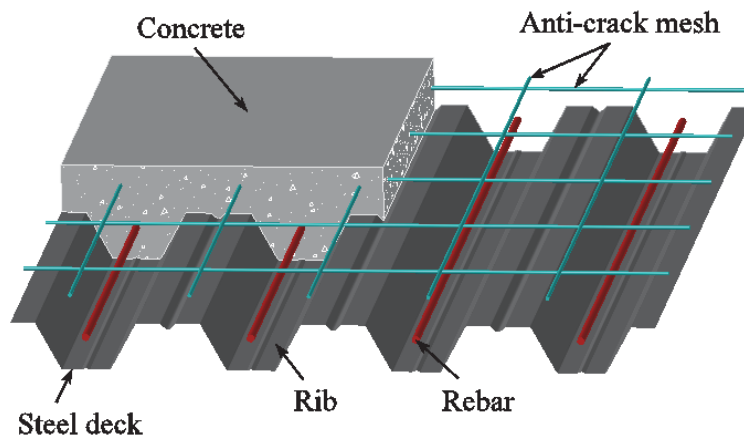


Figure 1. Typical layout of a composite slab with trapezoidal steel deck.

Since 1980, a significant increase in the use of composite slabs has taken place. The overall depth usually varies between 100 and 170 mm. Several types of steel deck are marketed in Europe, with a thickness varying between 0.7 and 1.2 mm, usually made from galvanized steel to increase durability [1].

Composite slabs have to meet fire-safety requirements in accordance to standards and regulations. Generally, standard fire tests using the standard fire curve ISO 834 [2] are utilized for determining the fire rating of this structural element, accounting for Load Bearing (R), Integrity (E) and Insulation (I).

In recent years, several studies have been conducted in order to evaluate the fire resistance of this type of structural element. In 1983, recognizing the need for calculation rules, the European Convention for Constructional Steelwork (ECCS) published the first instructions applied to the design of composite slabs with profiled steel deck when exposed to standard fire conditions. This technical note introduced simple calculation rules which were based on the results of fire tests performed on different European laboratories. According to this document, the explicit fire design is not required when the fire requirements are smaller or

equal to 30 minutes. The rules should only be applied to slabs which were properly designed to run at room temperature. At this time, the knowledge around the fire behaviour of composite slabs was incomplete and conservative assumptions were adopted. Therefore, the application of these recommendations may result on uneconomical solutions. According to this technical note, if the insulation criterion for fire resistance is fulfilled, then the integrity criterion is also fulfilled.

In 1990, Hamerlinck et al. [3] developed a thermal and mechanical numerical model with the objective of studying the influence of fire exposure on the performance of reinforced composite slabs. Both models were experimentally verified with loaded and unloaded tests. Concerning galvanized steel decks, due to the melting of the zinc layer and surface blackening, the resulting emissivity of the steel deck was calculated as function of the temperature. Simplifications were used for the thermal properties of the materials. Nevertheless, it was concluded that the numerical models satisfactorily predicted the behaviour of the tested slabs.

In 1991, within the scope of the first phase of the ECSC research project, Hamerlinck [1] performed an investigation regarding the mechanical and thermal behaviour of reinforced composite slabs under fire conditions. The study took into consideration the most important parameters for fire resistance and a new computer program was developed, enabling simulations at low computational cost. The developed two-dimensional model provided satisfactory results although not including three-dimensional thermal effects.

In 1999, Bailey et al. [4] published a study concerning the details and results of two experimental fire tests performed on a full-scale eight-storey building at the Building Research Establishment (BRE) Cardington Laboratory, UK. It was observed that the performance of the structure under fire conditions differed from what was expected from fire codes and calculation rules were usually conservative. In addition, both tests demonstrated that the behaviour of the structural element was different from what was normally observed in standard small-scale fire tests and no collapse occurred during the tests.

In 2002, Lim et al. [5] performed six fire tests on large-scale concrete slabs, comprising three reinforced concrete flat slabs and three composite steel-concrete slabs. The main objective of the tests was to investigate the fire behaviour of unrestrained simply supported slabs in a controlled furnace. The slabs were subjected to a live load and standard fire conditions during three hours. All the slabs resisted the full duration of the tests without collapsing, despite presenting extensive surface cracking on the unexposed surface and large deflections (up to 270 mm). In general, the measured fire resistance was higher than the predictions from normative recommendations. The tests evidenced the important effect of membrane action on preserving the structural stability of the slabs under fire exposure.

In 2011, Guo and Bailey [6] executed an experimental investigation with the objective of providing more insight on the behaviour of composite slabs during heating and cooling phases of fire. Nine equal composite slab specimens were tested: two of them at room temperature and the other ones at three different fire scenarios, which were controlled by burners and fans within the furnace. The specimens were loaded with representative values found in practice to investigate the structural behaviour. The results showed that the maximum temperature and both heating and cooling rate strongly affected the slab behaviour. For all slabs, the maximum

temperatures at the unexposed side and on the mesh were both higher during the cooling stages, due to the thermal inertial effect, which highlighted that insulation failure is likely to occur not only during heating but also during cooling phase.

In 2017, four full-scale fire tests were carried out by Guo-Qiang Li et al. [7] on composite slabs with profiled steel deck. The main objective of this investigation was to study the influence of the boundary conditions, reinforcement location, slab layout as well as the effect of unprotected secondary beams on tensile membrane action. The results revealed that the temperatures of the furnace were below the standard fire curve ISO 834. A comparison between experimental results and Eurocode 4 provisions showed that the simple calculation method for fire resistance results on conservative assumptions. Concerning the mechanical behaviour, the tensile membrane action provided a considerable contribution to the load bearing capacity. During the tests, significant debonding between the steel deck and concrete topping was observed.

In 2019, Jian Jiang et al. [8] from the National Institute of Standards and Technology (NIST) conducted a numerical investigation around different parameters that may influence on the fire resistance of composite slabs with respect to the thermal insulation criterion. An improved algebraic expression for the calculation of the fire resistance that explicitly accounts for moisture content of concrete was proposed. The formulation is valid for the calculation of the insulation fire resistance and applicable to an extended range of slab geometries in comparison to the limitations of the calculation method present in the current version of Eurocode 4. A set of 54 different composite slabs was selected for two-dimensional numerical analysis using a high-fidelity finite element approach. It was concluded that the concrete thickness and the moisture content were the parameters that most influenced the fire resistance. The proposed expression for fire resistance was validated against additional analyses and experimental data, resulting on maximum deviations of 15 and 18 minutes, respectively.

In this investigation, the focus is placed on three-dimensional numerical simulations using the standard fire curve ISO 834 in order to evaluate both load bearing fire resistance (R) and thermal insulation fire resistance (I). Three-dimensional mechanical and thermal analyses were developed using ANSYS to investigate the thermal effects of standard fire exposure. Concerning the thermal model, an air gap with constant thickness is included between the steel deck and concrete topping with the aim of simulating the debonding effects. Effectively, previous investigations mention the separation between the steel deck and concrete, which creates a thermal resistance in this interface.

Both mechanical and thermal models are validated against experimental results published by Hamerlinck [1]. Finally, a comparison between the fire resistance obtained numerically, experimentally and using the Eurocode 4 calculation method is presented.

2. FIRE RESISTANCE CRITERIA

Structural elements need to meet fire-safety requirements according to building codes. For composite slabs, the requirements are normally specified by fire ratings of 30, 60, 90 min or more. The fire rating of this type of building elements is normally made using standard fire

tests [9, 10], and should consider the criterion of Integrity (E), Insulation (I) and Load Bearing (R). Generally, experimental tests are expensive and time-consuming. As an alternative solution, the fire resistance can be evaluated by means of numerical simulations or using simple calculation methods. The fire resistance of the composite slabs is defined with respect to standard fire exposure from below. In this study, the fire resistance is investigated with respect to both load bearing (R) and thermal insulation (I) criteria.

The integrity (E) is the capacity to withstand fire in one side and the assessment should be made on the basis of measuring cracks or openings in excess of given dimensions, or the ignition of a cotton pad, or sustained flaming on the unexposed side. For cast in situ composite slabs, the integrity criterion is normally satisfied provided that the joints are adequately sealed.

The insulation (I) is the ability to withstand fire in one side and the assessment shall be made on the basis of the average temperature rise on the unexposed face limited to 140 °C above the initial average temperature, or; made on the basis of the maximum temperature rise at any point limited to 180 °C above the initial average temperature.

The load bearing resistance for flexural loaded elements (R) is the ability to support the loading during the test and the assessment shall be made on the basis of limiting vertical displacement D ($D=L^2/400d$ [mm]), or limiting rate of vertical displacement ($dD/dt=L^2/9000d$ [mm/min]), being L the clear span of the testing specimen in millimetres and d is the distance from the extreme fibre of the cold design compression zone to the extreme fibre of the cold design tensile zone of the structural section, in millimetres.

3. SIMPLIFIED CALCULATION METHOD OF EUROCODE 4

A simplified method is presented in the Annex D of EN 1994-1-2 [11] for the estimation of the fire resistance of unprotected composite slabs subjected to fire exposure from below according to the standard fire curve ISO 834. The analytical expressions present in the current version of this standard are based on the research conducted by Both [12] in 1998. During the last years, no revisions were made to these methods [8]. The fire resistance (t_i) with respect to thermal insulation criterion shall be determined according to equation (1).

$$t_i = a_0 + a_1 \cdot h_1 + a_2 \cdot \phi_{upper} + a_3 \cdot \frac{A}{L_r} + a_4 \cdot \frac{1}{l_3} + a_5 \cdot \frac{A}{L_r} \cdot \frac{1}{l_3} \quad (1)$$

The rib geometry factor (A/L_r) of the composite slab shall be calculated as follows:

$$A/L_r = h_2 \cdot ((l_1 + l_2)/2) / \left(l_2 + 2\sqrt{h_2^2 + ((l_1 - l_2)/2)^2} \right) \quad (2)$$

In addition to the geometric parameters of the composite slab, illustrated in figure 2, the fire resistance also depends on partial factors (a_i). Table 1 presents these factors for slabs with normal weight concrete (NWC).

a_0 (min)	a_1 (min/mm)	a_2 (min)	a_3 (min/mm)	a_4 (mm min)	a_5 (min)
-28.8	1.55	-12.6	0.33	-735	48.0

Table 1. Coefficients for determination of the fire resistance for NWC (adapted from EN 1994-1-2 [11]).

4. EXPERIMENTAL TESTS

An experimental test conducted by Hamerlinck [1] (test number 2) was selected to perform numerical simulations for both mechanical and thermal models. The slab was composed by the trapezoidal steel deck PRINS PSV 73 and a concrete topping with 70 mm thick using normal weight concrete. The simply supported slab was subjected to the ISO 834 standard fire. The profile of the composite slab is shown in figure 2.

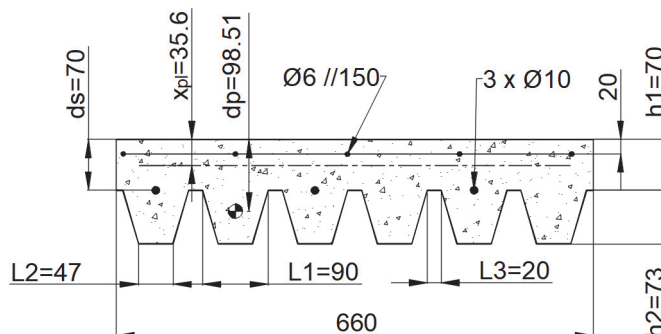


Figure 2. Profile of the tested slab: dimensions in millimetres (Hamerlinck [1]).

Normal weight concrete was used on the composite slab and the measured moisture content amounted to 3.5%.

5. NUMERICAL SIMULATIONS

In the following section, the methodology used to model and numerically determine the thermal and mechanical effects on the composite slab is presented. Therefore, a brief description of the finite elements, thermal/mechanical properties of materials, boundary conditions and convergence criterion is given for both thermal and mechanical model.

5.1. Thermal model

The composite slab is meshed in order to solve a nonlinear transient thermal analysis, using 3D models from ANSYS. The finite element method (FEM) requires the solution of equation (3) in the domain and the definition of the boundary conditions on equation (4) in the exposed and unexposed side of the slab.

$$\nabla(\lambda_{(T)} \cdot \nabla T) = \rho_{(T)} \cdot C_{p(T)} \cdot \partial T / \partial t \quad (3)$$

$$\lambda_{(T)} \cdot \nabla T \cdot \vec{n} = \alpha_c (T_g - T) + \phi \cdot \epsilon_m \cdot \epsilon_f \cdot \sigma \cdot (T_g^4 - T^4) \quad (4)$$

In the equations above: T represents the temperature of each material; $\rho(T)$ is the specific mass; $Cp(T)$ is the specific heat; $\lambda(T)$ is the thermal conductivity; α_c is the convection coefficient. T_g represents the gas temperature of the fire compartment, using the standard fire ISO 834 applied on the bottom part of the slab; ϕ is the view factor; ε_m is the emissivity of each material; ε_f represents the emissivity of the fire and σ represents the Stefan-Boltzmann constant.

The view factor (ϕ) quantifies the geometric relation between the surface emitting radiation and the surface receiving radiation. This factor depends on the surface areas and their orientations, as well as the distance between them [8]. The view factor of the lower flange of the composite slab is given as $\phi_{low} = 1$. Owing to the obstruction to direct exposure caused by the ribs of the steel deck, the view factor of the web and upper flange are smaller than one. This method of calculation is incorporated in EN 1994-1-2. The view factors for the upper flange (ϕ_{upper}) and web (ϕ_{web}) can be calculated as function of geometric parameters of the slab, according to the following equations.

$$\phi_{upper} = \frac{ad + cb - ab - cd}{2ab} = \frac{\sqrt{h_2^2 + \left(l_3 + \frac{l_1 - l_2}{2}\right)^2} - \sqrt{h_2^2 + \left(\frac{l_1 - l_2}{2}\right)^2}}{l_3} \quad (5)$$

$$\phi_{web} = \frac{ac + cd - ad}{2ac} = \frac{\sqrt{h_2^2 + \left(\frac{l_1 - l_2}{2}\right)^2} + (l_3 + l_1 - l_2) - \sqrt{h_2^2 + \left(l_3 + \frac{l_1 - l_2}{2}\right)^2}}{2\sqrt{h_2^2 + \left(\frac{l_1 - l_2}{2}\right)^2}} \quad (6)$$

The finite element method is applied to solve numerically the heat transfer equation using the software ANSYS. For an arbitrary composite slab with trapezoidal steel deck, the respective 3D mesh is presented in figure 3.

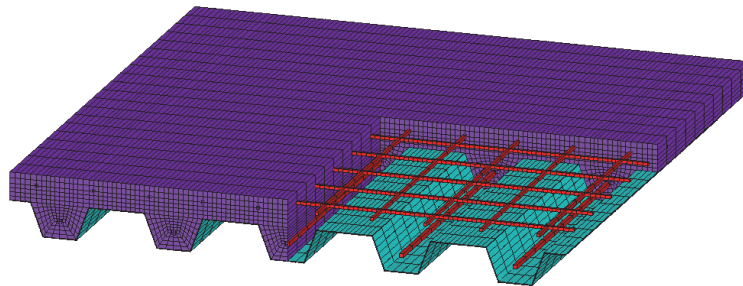


Figure 3. Finite element mesh of a composite slab with trapezoidal steel deck.

On the software, a three-dimensional model of the composite slab is introduced, which is composed by subdomains that correspond to the different materials, namely the concrete topping, the steel deck, the steel rebars and the steel mesh. A second alternative thermal model, using an air gap with a constant thickness (1 mm), is included between the steel

deck and the concrete topping in order to simulate debonding effects.

For each material, a specific 3D finite element is used. Three different finite elements are used: SHELL131, SOLID70 and LINK33. The SHELL131 element has four nodes with up to 32 degrees of freedom (temperature) per node, depending on the number of layers (one layer). This element presents linear interpolating functions in the plane of the element, using full Gauss integration method (2x2) and linear interpolating functions through the layer thickness (three Gauss points). The shell element is used to model the steel deck of the composite slab. The SOLID70 element presents eight nodes with a single degree of freedom (temperature) at each node. Linear interpolating functions are used for this element and the full Gauss integration method is also applied (2x2x2). This finite element is used to model the concrete topping and, in the second case, the air gap volume. The LINK33 element has two nodes with a single degree of freedom (temperature) per node. This uniaxial element presents linear interpolating functions as well as exact integration. The LINK33 element is used to model the anti-crack mesh and the rebars.

The thermal properties of the materials are temperature dependent and vary according to the standards used for composite slabs, steel structures and concrete structures [11, 13, 14]. The thermal properties of steel and concrete are presented in figures 4 and 5, respectively. The conductivity of steel decreases with temperature and the specific heat has a strong variation due to the allotropic phase transformation. Both density and conductivity of concrete decrease as the temperature increase. Regarding the conductivity, the upper limit was selected for the numerical simulations. The specific heat of concrete presents a peak value related to 3% of moisture content of concrete weight.

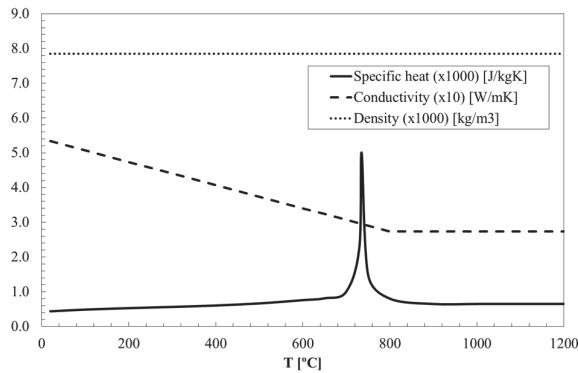


Figure 4. Thermal properties of carbon steel.

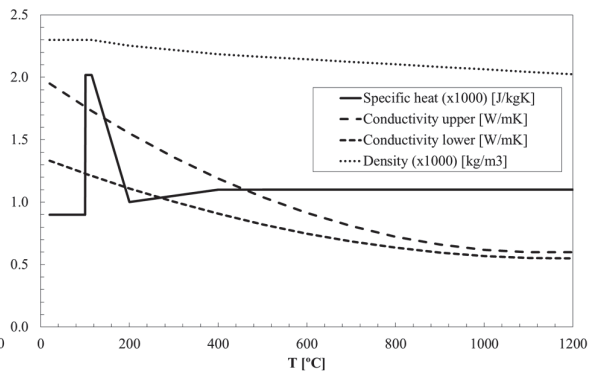


Figure 5. Thermal properties of concrete.

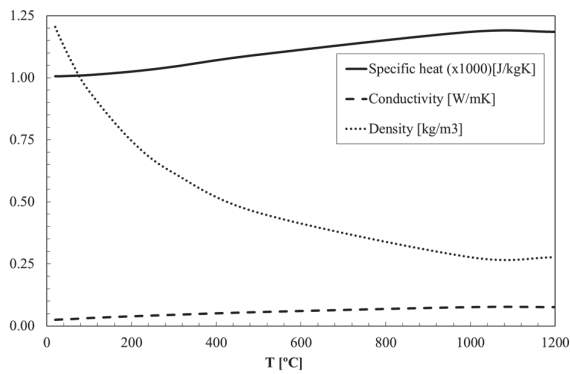


Figure 6. Thermal properties of air.

The thermal properties of air are depicted in figure 6. These properties are also temperature dependent and were used in the air gap to simulate the effects of debonding between the steel deck and the bottom surface of the concrete. This model only considers the heat flow by conduction in the air gap, due to the very small air gap thickness.

The exposed side of the slab is submitted to a heat flux by convection and radiation, see equation (4), using different values for view factors and a bulk temperature following the standard fire. The unexposed side is subjected to a convective heat flux (including the radiation heat flux), using a constant bulk temperature of 20 °C.

All the nodes of the numerical model are set with an initial condition for temperature of 20 °C. The lower part of the steel deck is subjected to standard fire conditions using a convection coefficient of 25 W/m²K and an emissivity of fire equal to 1. A convective coefficient of 9 W/m²K is applied on the upper part of the composite slab in order to include the radiation effect [15]. The main parameters of the applied boundary conditions are illustrated in figure 7.

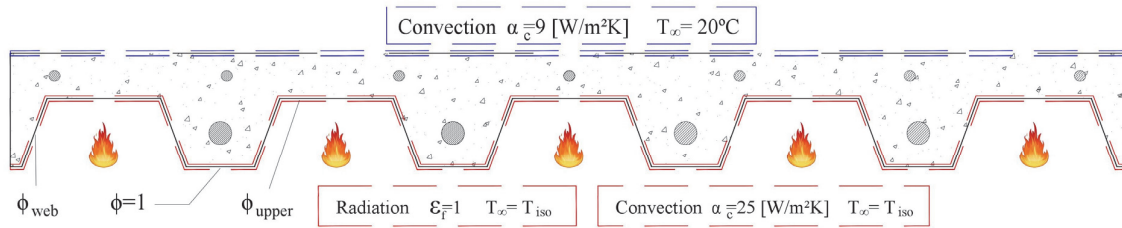


Figure 7. Representation of the applied boundary conditions.

The heat flow criterion was applied for the convergence criterion, using a tolerance value of 0.001 and a minimum reference value of 10^{-6} .

5.2. Mechanical model

The mechanical simulation for the fire behaviour of the composite slabs is also analysed. The model is validated using the experimental results from Hamerlinck [1]. The displacement and the rate of displacement are determined, compared with the experimental results and compared with the criterion for fire rating given by EN 1363-1 [10].

The integral value for the surface force over any surface of an arbitrary volume element within the material must sum to zero in order to keep the static equilibrium. Here we assume the existence of an external load $\{F\}$ (live and dead load) on material within the volume submitted to the stress field $[\sigma]$. The surface integral can be converted to a volume integral by the Gauss' divergence theorem. The final version of the equilibrium equation may be expressed in every cartesian coordinate, according to equation (7).

$$\nabla[\sigma] + \{F\} = \{0\} \quad (7)$$

The external load $\{F\}$ is considered to be constant under fire conditions. The load bearing capacity was determined for room temperature, using equation (8) for sagging moment resistance and assuming the neutral axis to be located above the steel deck. $M_{p,Rd}$ represents the plastic bending resistance, $N_{p,pl}$ the plastic tensile force for the effective section of the plate, $N_{s,pl}$ the plastic tensile force for rebars, d_p represents the centroidal position for the plate measured from the top of the cross-section, x_{pl} represents the position for the plastic neutral axis measured from the top and d_s represents the position of the rebars measured from the top.

$$M_{p,Rd} = N_{p,pl} \times \left(d_p - \frac{x_{pl}}{2} \right) + N_{s,pl} \times \left(d_s - \frac{x_{pl}}{2} \right) \quad (8)$$

The mechanical load is distributed over four lines of nodal loads, with a spacing of 800 mm. This load represents the live load (used as parameter). The dead load is included by means of inertial effect (2800 N/m^2). The composite slab is considered to be simply supported (restraining the displacements in vertical and out-of-plane directions at the left support and restraining all displacements in the right support). The lines of nodal forces were applied in accordance to the experimental setup, see figure 8.

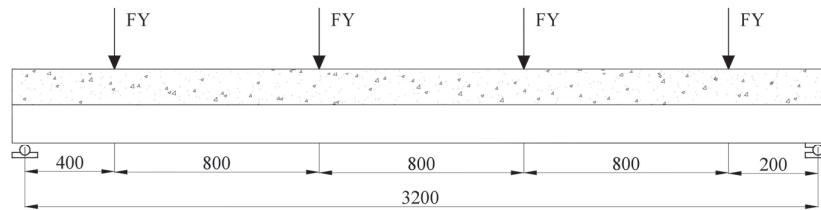


Figure 8. Representation of the mechanical model.

The dead load was calculated based on the volume and density of each material, using the inertial effect. The thermal load effect introduces the incremental time effect, using different files with the corresponding temperature field for each time step.

The finite element model uses a full three-dimensional finite element mesh, by switching the thermal SOLID70, SHELL131 and LINK33 finite element to the equivalent mechanical finite element SOLID185, SHELL181 and LINK180, see figure 9.

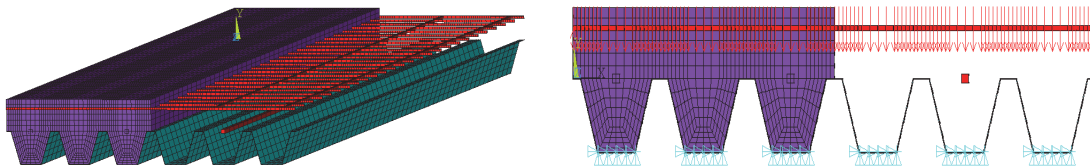


Figure 9. The finite element mechanical model.

SOLID185 is a three-dimensional finite element defined by eight nodes, having three degrees of freedom at each node (3 translations). This element uses linear interpolation functions and full gauss integration. SHELL181 is a four-node element with six degrees of freedom at each node (3 translations and 3 rotations). This element also uses linear interpolating functions for in-plane with full integration scheme and linear interpolating functions in-thickness direction with 3 integration points. LINK180 is a unidirectional finite element with 2 nodes and 3 degrees of freedom at each node (translations). This element is superposed to the concrete nodes and uses 1 integration point.

The incremental solution, based on Newton Raphson method is used with a convergence criterion defined by force and moment, for a tolerance value of 0.001 and a minimum reference value of 1. The elastic-plastic analysis was also used, considering the non-linear material properties of both materials, different thermal expansion between steel and concrete, see figure 10, and using the non-linear geometric analysis.

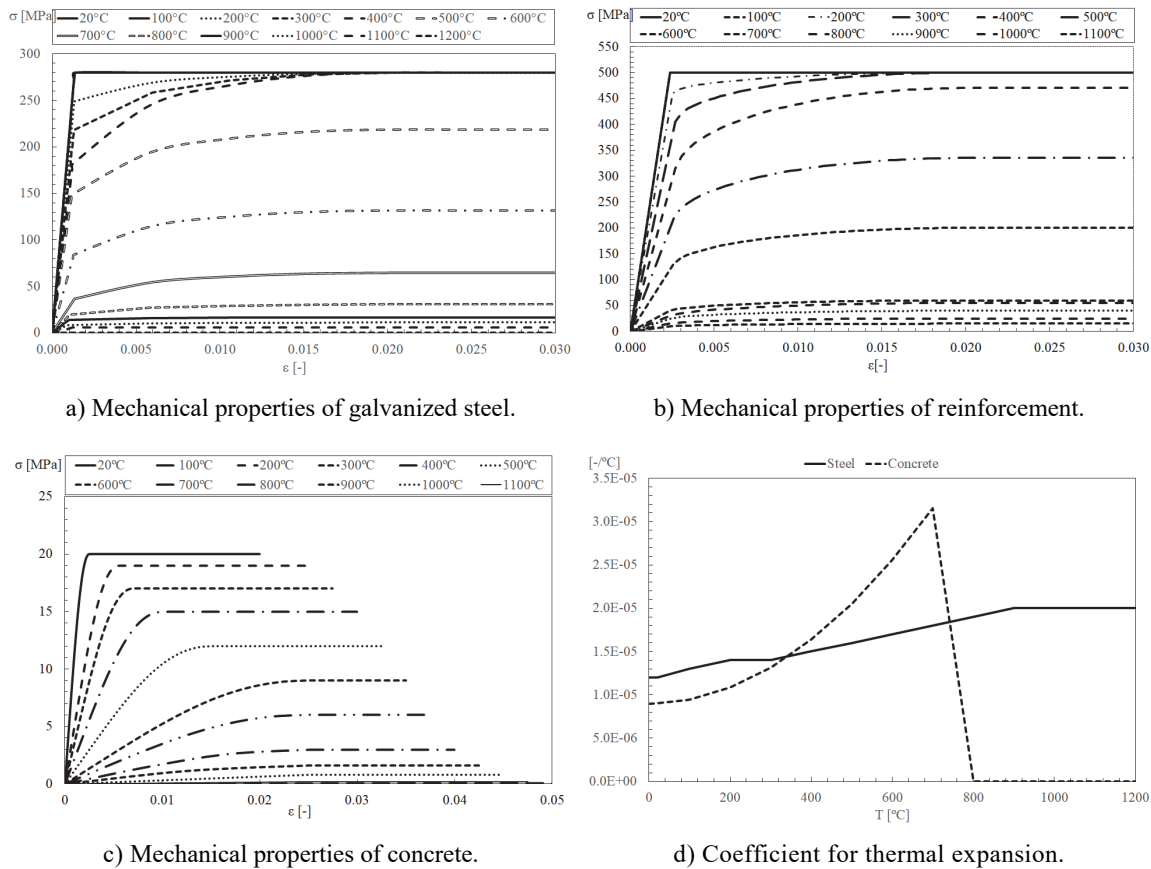


Figure 10. Mechanical properties for all materials.

The mechanical properties of the materials are temperature dependent and vary according to the standards used for composite slabs [11], steel structures [13] and concrete structures [14]. The thermal expansion for each material was also considered in the model, due to the existence of a very high temperature gradient through thickness. This gradient is responsible for the existence of thermal bowing, increasing the rotation of the cross-section. The change of thermal expansion with temperature, denoted as the coefficient of thermal expansion, is not constant, especially for concrete. Due to shrinkage, the expansion of concrete stops at elevated temperatures (beyond 650 °C). The expansion coefficient for steel has smaller variation with temperature. Changes in the microstructure explain the plateau between 750 and 800°C.

6. RESULTS

The results of the three-dimensional numerical simulations are presented in this section, resulting from the application of the preceding models. The thermal analysis presents the

results obtained with perfect contact and with an air gap 1 mm thick between the steel deck and the concrete topping. These thermal results are compared with experimental results. A comparison of the fire resistance between the numerical, experimental and simple calculation method results is also presented. The thermo-mechanical numerical results are also compared with the experimental results. A parametric analysis was also developed to determine the effect of the live load. A new proposal is presented for the fire resistance with respect to the load bearing criterion (R).

6.1. Thermal results

Figure 11 illustrates the temperature development (numerical and experimental) at different points as well as the average and maximum temperatures at the unexposed side of the slab. Analyzing the results, it can be observed that the temperature development on the selected points is quite similar between the experimental (EXPT) and the perfect contact model (NUM 0) at the first minutes of heating. Regarding the temperature development at point 2, the model with the air gap (NUM 1 – 1 mm) presents good approximation to the experimental results for temperatures over 100 °C. However, for the points 1 and 3, the perfect contact model presents better agreement with measured temperatures at the last minutes of heating. For the unexposed surface, the maximum and average temperature curves are very close for all the models. In this case, better agreement with the experimental results can be noticed using the model with the air gap.

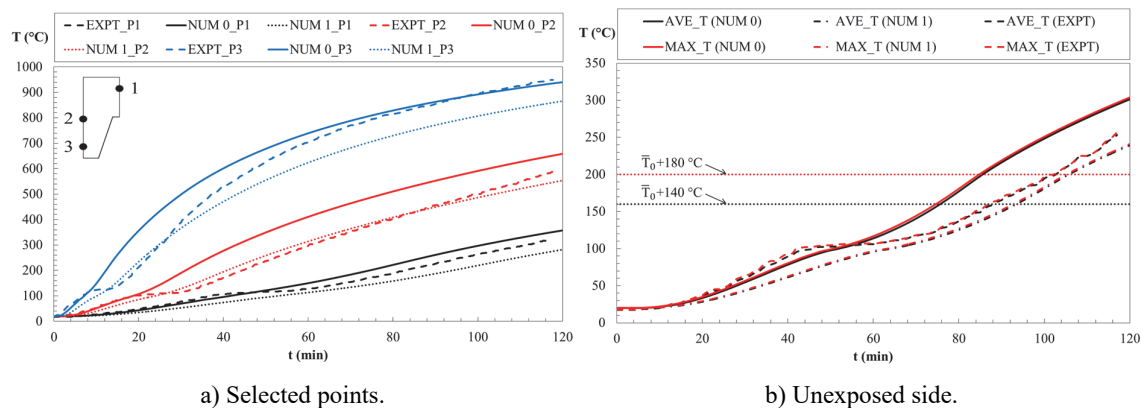


Figure 11. Comparison between numerical and experimental results. Point 1, 2 and 3 at distance 20, 74 and 123 mm from the top.

Table 2 presents the results obtained for the fire resistance (criterion “I”) of the slab with respect to the average temperature rise (t_{fi} Ave) and the maximum temperature rise (t_{fi} Max) at the unexposed surface. Obviously, for each model the lowest value between the two criteria governs the fire resistance.

	Model NUM 0	Model NUM 1	EXPT result	EN 1994-1-2 result
t_{fi} Ave (min)	75.6	93.5	88.2	106.5
t_{fi} Max (min)	84.8	105.1	102.1	

Table 2. Fire resistance for insulation condition: experimental, numerical and analytical results.

Assuming the experimental result as reference, it can be observed that the air gap model slightly overestimated the fire resistance, with a relative error of 6%. A bigger discrepancy is obtained using the perfect contact model, with a relative error of 14.3%. The EN 1994-1-2 provisions overestimated the fire resistance, providing an unsafe result with a relative error of 20.7%.

6.2. Mechanical results

In order to evaluate the fire resistance, the incremental and iterative solution is included. The maximum displacement and the rate of the maximum displacement should be analysed. Figure 12 represents the comparison between the experimental results and the numerical results. The critical time was determined by the first to archive the limiting conditions presented in EN1363-1[10].

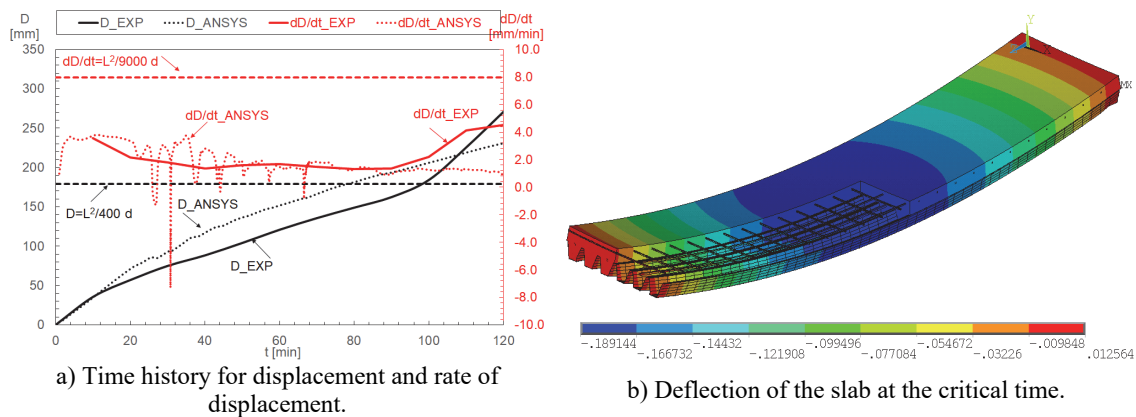


Figure 12. Analysis of the composite slab with a live load of 2.7 kN/m².

The vertical displacement of the slab changes with time. The curvature of the slab starts increasing rapidly and deflections increase accordingly. In a second stage, the deflection rate decreases as thermal curvature increases less. Near the ultimate limit state, the deflection rate increases again due to the plastic material behaviour.

For the mechanical analyses, it should be highlighted that the thermal load was determined based on the perfect contact model between materials (NUM 0). That is, the effect of the air gap between the steel deck and concrete was not taken into consideration. This fact results in higher temperature values for the materials and explains the higher predicted values for the vertical displacement of the numerical results.

Table 3 presents the comparison between the mechanical model with perfect contact and

experimental results concerning the load bearing fire resistance.

	Model NUM 0	EXPT result
$t_{fi} D$ (min)	78	97
$t_{fi} dD/dt$ (min)	Not achieved	Not achieved

Table 3. Fire resistance for load bearing condition: experimental and numerical results.

The difference between both results can be explained by several factors, mainly by the temperature field in each time step. Other parameters are also reported and are related with several phenomena during the test (variation of the view factors, creation of the air gap effect between the steel deck and concrete, restraint effect in the supports, direction of the applied load during the test, among others).

A parametric analysis was also developed, in order to verify the effect of the live load on the fire resistance. The load level, μ_0 , was determined by the ratio of the total load (live and dead) by the plastic load at room temperature, proposed by the EN 1994-1-1 [16]. The load varied from 1.0 kN/m² to 21.0 kN/m²

The fire resistance decreases with the load level, see figure 13. The critical temperatures of the steel components were determined based on the fire resistance criteria. These values also decrease with the load level. The fire resistance for load bearing criterion was exclusively governed by the critical displacement value (D). The rate of displacement (dD/dt) did not reach the critical value for load level values below $\mu_0=43\%$. For higher load levels, the critical displacement rate becomes important, but never anticipates the time for the critical displacement. The thermal gradient can be easily determined for each load level, being approximately equal to 700 °C/123 mm in the vertical direction. This value seems to be independent of the load level.

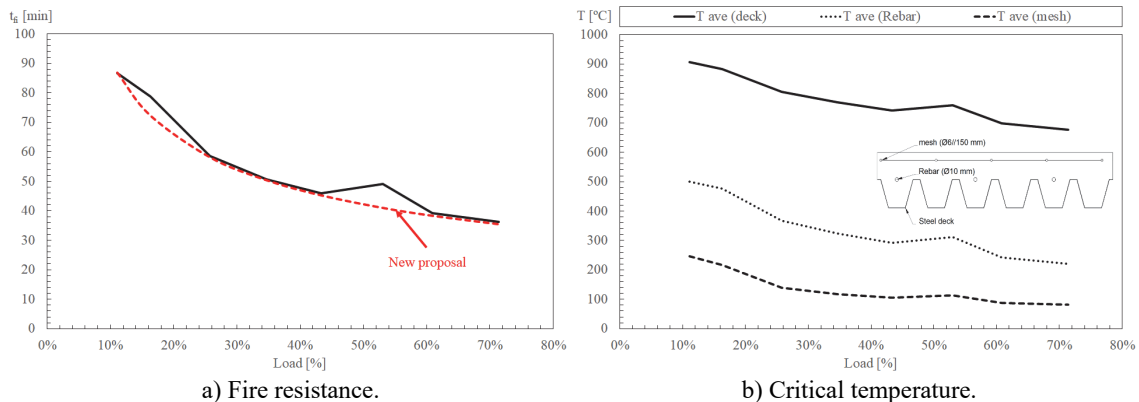


Figure 13. Fire resistance of the composite slab and critical temperature for the steel components.

The fire resistance was approximated with the minimum safety level, considering the results of the new proposal bellow the line of the numerical results. The new formula is presented in

equation 9.

$$t_{fi} = 32.104 \mu_0^{-0.464} - 2 \quad (9)$$

In practice, rebars should be applied to composite slabs with steel deck in cases when the required fire resistance time is higher than 30 minutes. When these elements are submitted to fire exposure, the contribution of the steel deck to the load bearing resistance decreases considerably, being part of this capacity transferred to the rebars.

7. CONCLUSIONS

This study presented the description of the thermal and mechanical three-dimensional finite element models as well as its validation against experimental data. The fire resistance according to the thermal insulation (I) and load bearing (R) criteria was determined and compared to experimental data as well as EN 1994-1-2 provisions. With the objective of simulating the effects of the debonding of the steel deck from concrete, an insulating layer (air gap) with a constant thickness of 1 mm was introduced between the concrete and steel deck. Regarding the experimental results for the temperature development, a plateau at about 100 °C (due to moisture evaporation) should be highlighted, resulting in a decrease in the rate of temperature increase. The numerical results do not present this pronounced plateau possibly because localized moisture concentrations in the test may be higher than the uniform moisture content introduced in the model.

The fire resistance with respect to the thermal insulation criterion was governed by the average temperature rise criterion for both thermal models (NUM 0 and NUM 1) as well as for experimental results. The perfect contact model underestimates the fire resistance. In general, the results obtained with the air gap model presented better agreement with experimental results and satisfactorily simulated the debonding effect, reducing the temperature rise at the selected points and unexposed side as well.

The EN 1994-1-2 provisions for the fire resistance according to thermal insulation criterion (I) was on the unsafe side, that is, the calculated fire resistance was greater than the measured one.

Using the perfect contact model (NUM 0), the fire resistance with respect to the load bearing criterion was governed by the maximum displacement criterion. The numerical result underestimated the fire resistance due to the higher temperature field achieved with this model.

The fire resistance decreases with the load level and a new proposal is presented. More numerical simulations are expected soon, which should be validated with other studies to verify this first approaching formula.

REFERENCES

- [1] A. F. Hamerlinck, "The behaviour of fire-exposed composite steel/concrete slabs," Eindhoven University of Technology, 1991.
- [2] International Standard ISO 834, "Fire-resistance tests - Elements of building construction." 1975.

- [3] R. Hamerlinck, L. Twilt, and J. W. B. Stark, “A numerical model for fire-exposed composite steel/concrete slabs,” *10th Int. Spec. Conf. Cold-Formed Steel Struct. - Int. Spec. Conf. Cold-Formed Steel Struct.* 5, pp. 115–130, 1990.
- [4] C. G. Bailey, T. Lennon, and D. B. Moore, “The behaviour of full-scale steel-framed buildings subjected to compartment fires,” *Struct. Eng.*, vol. 77, no. 8, pp. 15–21, 1999.
- [5] L. Lim and C. Wade, “Experimental fire tests of two-way concrete slabs,” Christchurch, 2002.
- [6] S. Guo and C. G. Bailey, “Experimental behaviour of composite slabs during the heating and cooling fire stages,” *Eng. Struct.*, vol. 33, pp. 563–571, 2011.
- [7] G.-Q. Li, N. Zhang, and J. Jiang, “Experimental investigation on thermal and mechanical behaviour of composite floors exposed to standard fire,” *Fire Saf. J.*, vol. 89, no. November, pp. 63–76, Apr. 2017.
- [8] J. Jiang, A. Pintar, J. M. Weigand, J. A. Main, and F. Sadek, “Improved calculation method for insulation-based fire resistance of composite slabs,” *Fire Saf. J.*, vol. 105, pp. 144–153, Mar. 2019.
- [9] CEN - European Committee for Standardization, *EN 1365-2: Fire resistance tests for load bearing elements - Part 2: Floors and roofs (Withdrawal)*. Brussels, 2014.
- [10] CEN- European Committee for Standardization, *EN 1363-1: Fire resistance tests Part 1: General Requirements*, CEN-Europ. Brussels: CEN- European Committee for Standardization, 2012.
- [11] CEN- European Committee for Standardization, *EN 1994-1-2: Design of composite steel and concrete structures. Part 1-2: General rules - Structural fire design*. Brussels: CEN- European Committee for Standardization, 2005.
- [12] C. Both, “The fire resistance of composite steel-concrete slabs,” Technical University of Delft, 1998.
- [13] CEN- European Committee for Standardization, *EN 1993-1-2: Design of steel structures - Part 1-2: General rules - Structural fire design Eurocode*. Brussels: CEN - European Committee for Standardization, 2005.
- [14] CEN- European Committee for Standardization, *EN 1992-1-2: Design of concrete structures - Part 1-2: General rules - Structural fire design*, vol. EN 1992. Brussels: CEN - European Committee for Standardization, 2004.
- [15] CEN- European Committee for Standardization, *EN 1991-1-2, Eurocode 1: Actions on structures – Part 1-2: General actions – Actions on structures exposed to fire*. Brussels: CEN- European Committee for Standardization, 2002.
- [16] CEN- European Committee for Standardization, *EN 1994-1-1: Design of composite steel and concrete structures - Part 1-1: General rules and rules for buildings*. Brussels: CEN - European Committee for Standardization, 2004.

Author Index

- Afonso, A, 375
Afonso, M, 337
Afonso, O, 273
Aguiar, M, 417
Aguiar-Contraria, I, 137
Alexandrov, A, 363
Andraz, J, 321, 343
Arantes, M, 181
Atanassov, K, 363, 397
Atanassova, L, 397
Atanassova, V, 199, 251
- Balsa, C, 119
Barbeiro, S, 501
Barbosa, I, 7
Barbosa, J I, 587
Barbosa, M, 457, 545
Belinha, J, 415, 437, 441, 457, 499,
505, 545
Benlakehal, N, 17, 27
Bordas, S, 1
Bougara, A, 17, 27
Braga, V, 507, 509
Bureva, V, 397
- Céspedes, J, 441
Candeias, R, 343, 357
Cardoso, S, 61
Carvalho, Alda, 7, 487, 547, 573
Carvalho, André, 7, 587
Casaca, C, 547
Clain, S, 447
Conceição, A, 301, 321, 343
Correia, A, 507, 509
- Correia, L, 357
Costa, F, 533
- Delkov, A, 397
Delkov, A, 215
Dias, M, 509
Dinis, L, 415, 437, 457
Doukovska, L, 251
Doukovska, L, 199
- Escobar, J, 517
- Falcão, M, 139, 141
Fellouh, A, 17, 27
Ferrás, L, 375, 565, 567
Ferreira, C, 377
Ferreira, M, 503
Flores-Garrido, J, 445
Fonseca, E, 109
Fontes, F, 533, 541
Ford, N, 565, 567
Forouzandeh, Z, 541
Francisco, R, 503
- Galán, J, 445
Gama, S, 337, 543
Gavina, A, 479
Gomes, J, 505
Guerra, A, 499
- Jorge, R N, 415, 437, 441, 457, 499,
505, 545
- Kimura, É, 119, 139, 141
Krowiak, A, 85, 97



SYMCOMP2019
ECCOMAS Thematic Conference